粒度構成がマグクロれんがの物性に与える影響

Influence of particle size distribution on the properties of magnesia-chrome bricks

岸本一輝*，清水公一**，後藤　潔***

Kazuki KISHIMOTO*, Koichi SHIMIZU** and Kiyoshi GOTO***

要　旨

マグクロれんがの粒度構成，つまり粗粒・中粒・微粉の割合を系統的に変えて作成した焼成体の微構造，比重，強度，気孔径分布，そして耐熱衝撃性などの物性への影響を調査したところ , 微粉割合の増加に伴い焼結性の増進による緻密化や強度が向上した。一方 , 粗粒割合の増加に伴い , 焼成時粗粒周囲に形成される空隙による，弾性率低下が見られた。また、今回検討した粒度構成において耐熱衝撃性に及ぼす影響は明確に示すことができなかった。

Abstract

In magnesia-chrome bricks with adjusted systematically the particle size distribution of coarse, medium, and fine particles, microstructure, bulk specific gravity, strength, pore size distribution and thermal shock resistance were investigated in their fired state. The distribution with increased the fine particle derived a structural densification with strengthening mechanically by improving a sinterability of the bricks during firing. On the other hand, the distribution with increased the coarse particle made the decrease in the modulus of elasticity by forming voids around the coarse grain during firing. No correlation was observed in the thermal shock resistance of the fired bricks with the particle size distribution in the raw powder processing examined.

1　緒言

マグクロれんがは高温下における安定性に優れることから，各種窯炉，特に二次精錬炉の内張耐火物として広く使用されている。二次精錬炉に使用されるマグクロれんがの損傷形態には，熱的・機械的スポーリング，スラグによる化学的侵食，溶鋼･スラグの流動による摩耗などがあり，耐火物にとって非常に過酷な使用環境と言える[1)]。これらの損傷に対して，れんがの粒度構成が大きく影響すると考えられ，粒度構成の検討は過去の報告においてもなされている[2)]。しかし，粗粒・中粒・微粉割合を系統的に変化させた報告例はあまりない。今回の報告では，特定の粒度割合のみを変えるのではなく，粗粒・中粒・微粉の割合を系統的に変えて粒度構成がマグクロれんがの物性に与える影響

1 Introduction

Magnesia-chrome bricks are widely used as lining for various metallurgical furnaces such as those used for secondary refining of steels, due to their excellent stability at high temperatures. The wear patterns of the magnesia-chrome bricks used in the secondary refining furnaces include thermal and mechanical spalling, corrosion by slag, and erosion by molten steel and slag flows, which can be said to be a quite severe usage environment for refractories[1)]. It is believed that the particle size distribution of the bricks greatly affects these damages by the wear, and the study of particle size distribution has been previously reported[2)]. However, there are no reports where the distribution of coarse, medium, and fine particles were systematically varied.

In this study, we investigated the effect of particle size distribution on the properties of magnesia-chrome bricks by systematically changing the ratio of coarse, medium, and fine particles, rather

＊　技術研究所 製品プロセス研究センター　Product R&D Center, Technical Research Institute
＊＊　技術研究所 製品プロセス研究センター センター長　Center Manager, Product R&D Center, Technical Research Institute
＊＊＊　フェロー 技術研究所 所長　Fellow, General Manager, Technical Research Institute

を調査した。

2　実験方法

2・1　試作内容

試作れんがには，焼結マグネシアとクロム鉱を各配合の各粒度域において体積割合で 50 ％ずつ使用し，酸化クロムを各れんがに同量ずつ添加した。焼結マグネシアとクロム鉱の各粒度毎の割合は**表 1** 及び**図 1** に①～⑨で示す粒度構成になるように調整した。それぞれの配合を同一圧で並形れんがに成形後，乾燥工程を経て，焼成を行った。

2・2　試験方法

焼成体において見掛気孔率，かさ比重，音速弾性率，冷間圧縮強さ，1480 ℃における曲げ強さ，気孔径分布，組織観察，耐熱衝撃性などの評価

than changing only specific particle size ratio.

2 Experimental method

2･1 Test bricks

For the test bricks, sintered magnesia and chromite were used in equal volume ratios of 50% each, in each composition and each particle size range, and the same amount of chromium oxide was added to each brick. The ratio of each particle size of sintered magnesia and chromite was adjusted to match the particle size distribution shown in **Table 1** and **Fig. 1** as ① to ⑨. Each mixture was molded into standard type (230x100x100mm) bricks of the same shape and pressure, then went through a drying process, and was fired.

2･2 Test method

Tests were conducted on the fired body for apparent porosity, bulk specific gravity, modulus of elasticity, cold crushing strength, modulus of rupture at 1480 ℃, pore size distribution, microstructure

Table 1 Particle size distribution of brick mixtures ① to ⑨ for magnesia-chrome brick

Particle size distribution		①	②	③	④	⑤	⑥	⑦	⑧	⑨
Chromite 50 % - sintered MgO 50 %										
Particle size	Coarse	55	55	55	45	45	45	35	35	35
	Medium	35	27.5	20	45	37.5	30	55	47.5	40
	Fine	10	17.5	25	10	17.5	25	10	17.5	25

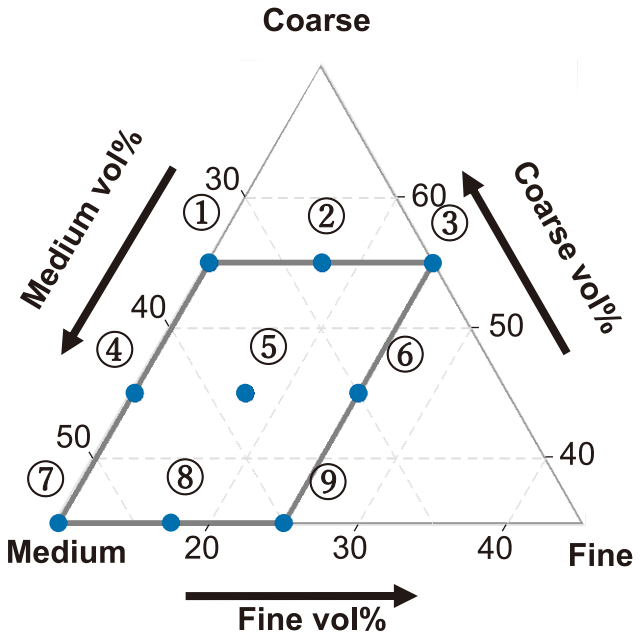

Fig. 1 Raw material particle size distribution of test bricks in the triangle diagram.

を行った。

耐熱衝撃性は 1 辺 50 mm の立方体に切り出した試験片を 1400 ℃に保定した電気炉内に 15 min 間挿入した。その後電気炉から取り出し，30 ℃以下の循環水の水槽の中に浸し，3 min 間冷却した。その後水槽から取り出し，12 min 間自然冷却を行った。この加熱 - 水冷 - 空冷のサイクルを繰り返し，剥落するまでのサイクル数で耐熱衝撃性を評価した。

2・3　試験結果の解析方法

今回の検討では，粗粒・中粒・微粉割合が各物性に与える影響を明らかにするために選ばれた**表 1・図 1** に示した①～⑨に示す材料において 2・2 に述べた各種試験における評価結果を得た。そしてこれらの結果を用いて実験計画法の混合計画を適用し，各評価物性毎に混合等高線プロットを作成し，粒度構成の及ぼす影響を可視化するとともに R^2 を求め粒度構成との相関性を示した。

3　結果

焼成体のかさ比重及び気孔率の混合等高線プロットをそれぞれ**図 2** 及び **3** に示している。粒度

observation and thermal shock resistance.

The thermal shock test was performed in the cycle of heating a test piece with 50 mm cube inserted into an electric furnace maintained at 1400 ℃ for 15 min, quenching in a circulating water tank at temperature below 30 ℃ for 3 min after removal from the furnace, and cooling in air for 12 min finally after picking up from the water tank. In the heat cycle performed, the thermal shock resistance was determined by the number of cycles to spall.

2･3 Analytical method of the test results

The effects of distribution of coarse, medium, and fine particles on various properties were checked in the fired state of the materials (①～⑨) indicated in **Table 1** and **Fig. 1**. Using the results obtained from the various tests mentioned above, the mixture design of the design of experiments was applied, to draw contour lines on a triangle map shown in **Fig. 1** for the various properties determined in the tests. This allows to visualize the effect of particle size distribution on the properties of the fired state and to correlate them by calculating R^2. Where, R is correlation coefficient in regression analysis and R^2 is coefficient of determination obtained by multiple regression analysis.

3 Results

The triangle contour plots of the bulk specific gravity and porosity of the fired body are shown in

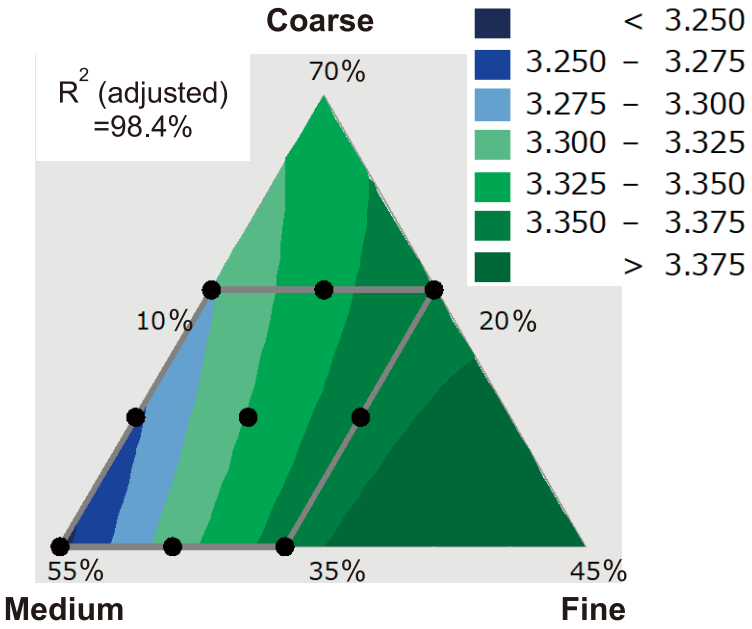

Fig. 2 Influence of particle size distribution on bulk specific gravity with triangle contour map.

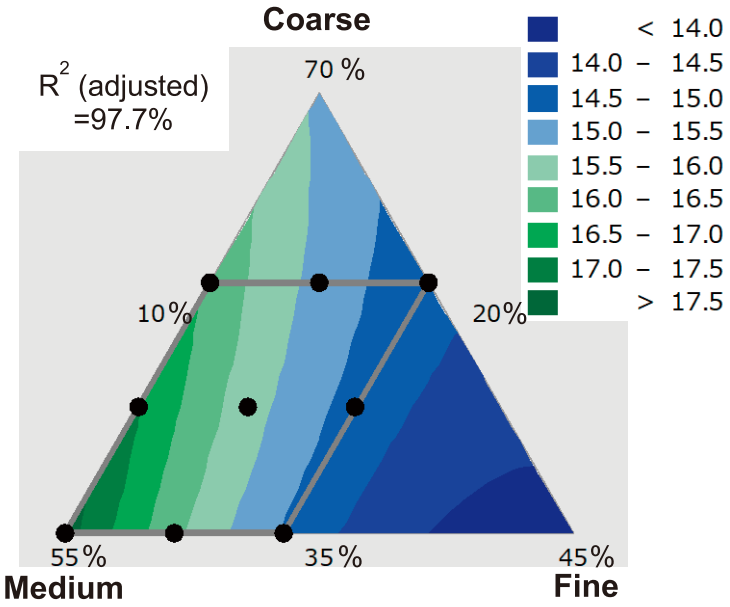

Fig. 3 Influence of particle size distribution on apparent porosity with triangle contour map.

構成の変化に伴い両方の値が以下に述べるように変化している。同じ粗粒割合 55% で微粉割合を 10 から 25% に増加した場合，つまり，**図 1** において①から③へと粒度構成を変化させた場合，かさ比重は 3.30（3.275-3.300 の領域）から 3.36（3.350-3.375 の領域）に増加し，見掛気孔率は 16.4%（16.0-16.5 の領域）から 14.8%（14.5-15.0 の領域）に低下している。また，同じ微粉割合 10% で粗粒割合を 35 から 55% に増加した場合，つまり，**図 1** において⑦から①へと粒度構成を変化させた場合，かさ比重が 3.24（< 3.250 の領域）から 3.30（3.275-3.300 の領域）に増加し，見掛気孔率は 17.7%（> 17.5 の領域）から 16.4%（16.0-16.5 の領域）に低下している。

図 4 に微構造写真を示す。写真の各領域は，その輝度によって大まかに別けることができる。つまり，最も輝度が高い部分がクロム鉱，次に輝度が高い部分が焼結マグネシア，そして最も輝度が低い（暗い）部分が空隙をそれぞれ示している。粗粒割合が同じで微粉割合が異なる 3 つの組み合わせ，つまり，**図 1** に示す三角図で 3 つの水平軸①～③，④～⑥，そして⑦～⑨のそれぞれにおいて

Figs. 2 and **3**, respectively. When the ratio of fine particle was increased from 10 to 25% at the same coarse particle ratio of 55%, corresponding to the particle size distribution change from ① to ③ in **Fig. 1**, the bulk specific gravity increased from 3.30 (the range of 3.275-3.300) to 3.36 (the range of 3.350-3.375), and the apparent porosity decreased from 16.4 (the range of 16.0-16.5) to 14.8% (the range of 14.5-15.0). Also, when the coarse particle ratio was increased from 35 to 55% at the same fine particle ratio of 10%, the particle size distribution change from ⑦ to ① in Fig. 1, the bulk specific gravity increased from 3.24 (less than 3.250) to 3.30 (the range of 3.275-3.300), and the apparent porosity decreased from 17.7 (more than 17.5) to 16.4% (the range of 16.0-16.5).

Figure 4 shows micrographs of the fired state of the materials with particle size distributions ① to ⑨. In the micrographs, the area indicating the components was distinguished roughly by their brightness, as the brightest chromite, the least(darkest) void and the intermediate magnesia. The decrease in the void with increase in the ratio of fine particle is confirmed in the three combinations with the same coarse particle ratio of the three horizontal axes ① to ③, ④ to ⑥, and ⑦ to ⑨, respectively, in the triangle diagram shown in **Fig. 1**. Such a clear difference, however, is not observed in the three combinations of the different coarse particle ratio with the same fine

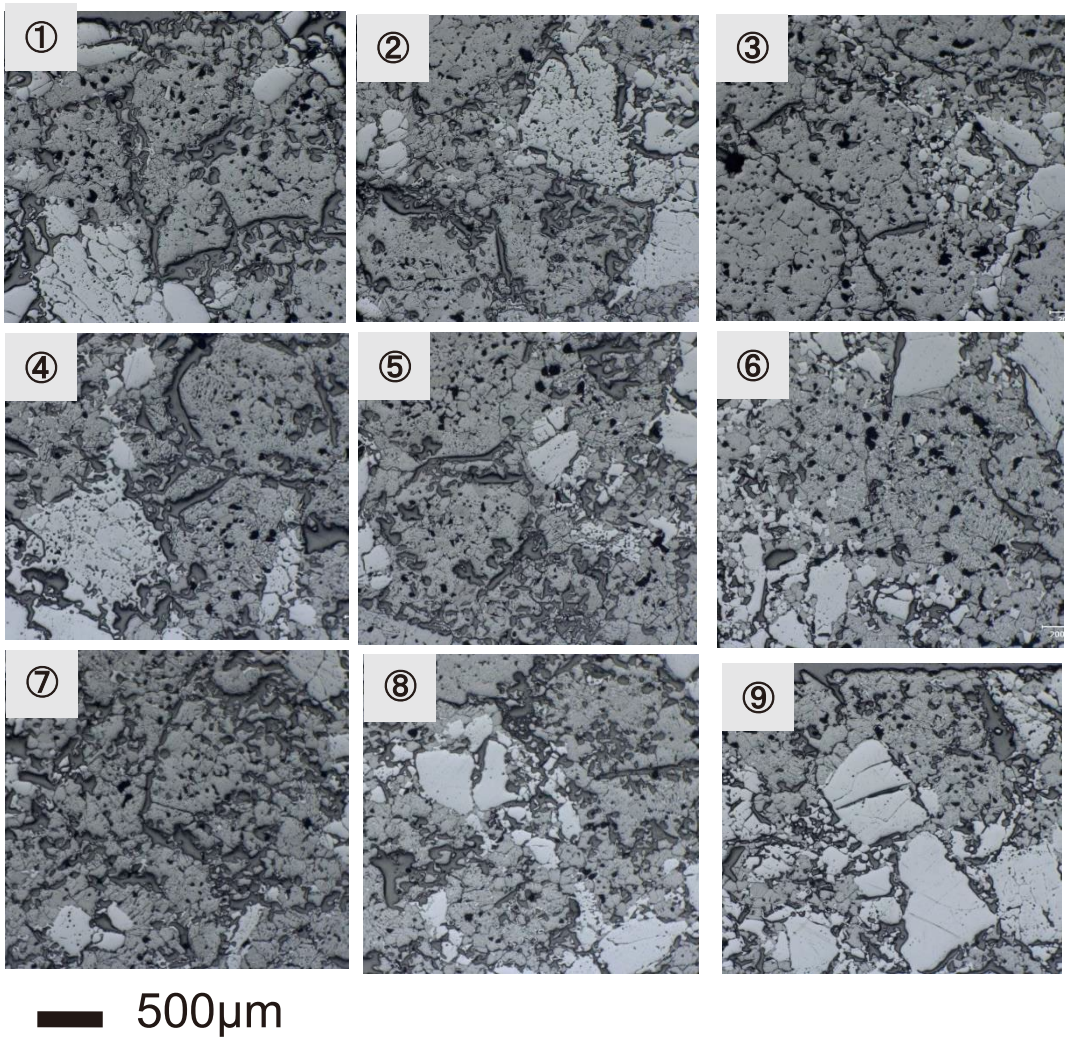

Fig. 4 Comparison of microstructures in fired materials with particle size distribution of ① to ⑨.

Table 2 Test results of the fired materials with particle size distribution ① to ⑨

Particle size distribution	①	②	③	④	⑤	⑥	⑦	⑧	⑨
Bulk Specific gravity / -	3.30	3.34	3.36	3.27	3.32	3.37	3.24	3.32	3.36
Parcentage dimentional change / %	1.30	0.69	0.31	1.44	0.76	0.26	1.29	0.81	0.24
Apparent porosity / %	16.4	15.3	14.8	17.1	15.9	14.6	17.7	16.0	15.1
Integrated porous volume / ml･g^{-1}	0.046	0.039	0.037	0.050	0.043	0.037	0.049	0.046	0.042
Integrated porous volume / ml･g^{-1}(≦10μm)	0.009	0.011	0.012	0.012	0.012	0.012	0.009	0.010	0.014
Modulus of elasticity,E / GPa	37	35	39	41	45	51	46	50	46
Cold crushing strength / MPa	66	80	83	78	87	97	74	93	95
Hot modulus of rupture at 1480℃,S / MPa	6	8	9	9	9	10	7	8	9
E/S^2 (x10^{-3}Pa^{-1}).	0.9	0.6	0.4	0.5	0.5	0.6	0.9	0.7	0.6
Number of cycle to spall	8	7.5	8.5	7.5	8.5	8	8	7.5	9

微粉割合の増加に伴い，空隙が少なくなっていることが分かる。一方，微粉割合が同じで粗粒割合が異なる３つの組み合わせ，つまり，**図１**に示す三角図で３つの側面軸①④⑦，②⑤⑧，そして③⑥⑨のそれぞれにおいては大きな違いは見られない。**表２**に示した細孔容積の測定結果を基にした particle ratio of the three side axes ①④⑦, ②⑤⑧, and ③⑥⑨ in the triangle diagram. The triangle contour plots based on the measured results of pore volume shown in **Table 2** are expressed in **Fig. 5**. They show decrease in pore volume with increase in the ratio of coarse and fine particles, indicating a strong correlation with the particle size distribution.

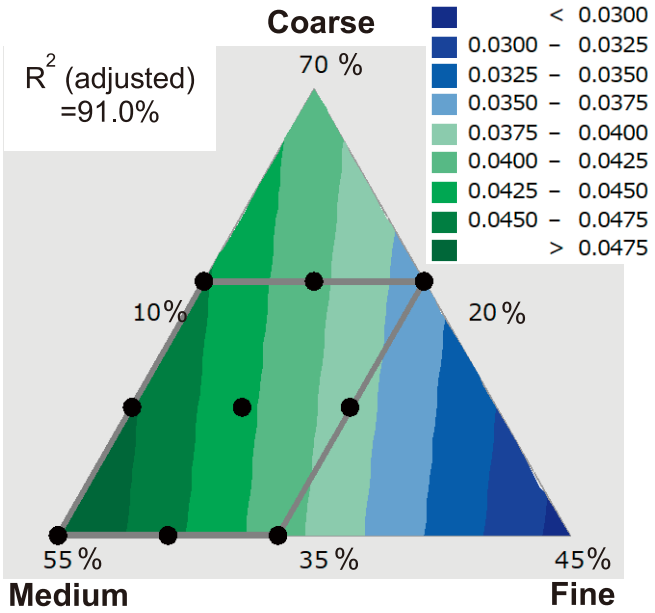

Fig. 5 Influence of particle size distribution on integrated porous volume with triangle contour map.

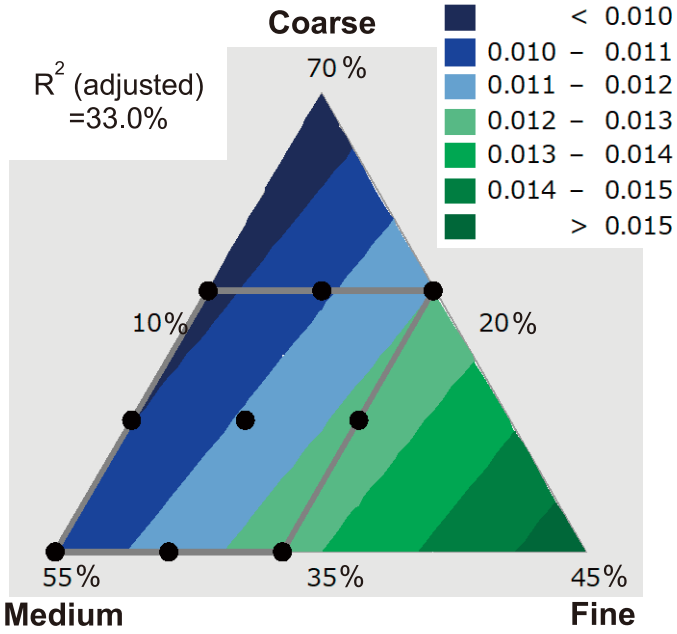

Fig. 6 Influence of particle size distribution on integrated porous volume (≦10μm) with triangle contour map.

混合等高線プロットを**図 5** に示している。粗粒・微粉割合の増加に伴う細孔容積の低減を示し，粒度構成との高い相関性を示している。しかし，**図 6** に示している 10 μm 以下の細孔容積についての混合等高線プロットでは粒度構成との相関性が低いことを示している。従って 10 μm 以上の比較的大きな細孔容積が微粉割合の増加に伴い低減していることが分かる。

However, the contour plots of the volume of pore less than 10 μm indicate a weak correlation with the particle size distribution as shown in **Fig. 6**. Therefore, it can be seen that the volume of relatively large pore with 10 μm or more is decreasing with the increase in the ratio of fine particle.

Figure 7 shows a triangle contour plot of the cold crushing strength which increases with increasing in the ratio of fine particle. Actually, at the same coarse particle ratio of 45%, when the fine

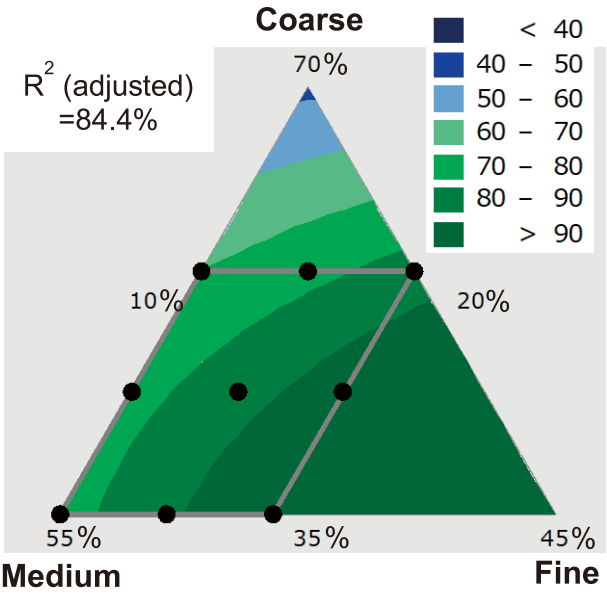

Fig. 7 Influence of particle size distribution on cold crushing strength with triangle contour map.

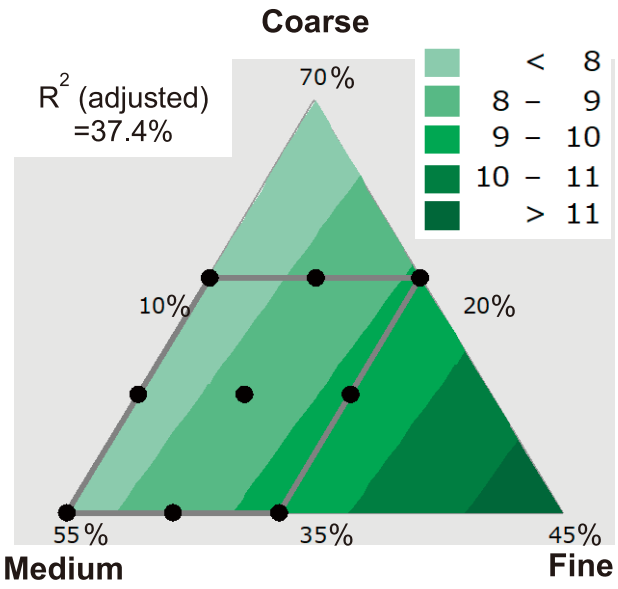

Fig. 8 Influence of particle size distribution on modulus of rupture at 1480℃ with triangle contour map.

図 7 に冷間圧縮強さの混合等高線プロットを示す。微粉割合の増加に伴い，上昇している。同じ粗粒割合 45% で微粉割合の影響を見ると微粉が④から⑥に増加した場合，圧縮強さは，78 MPa（70-80 の領域）から 97 MPa（＞ 90 の領域）に上昇している。また，**図 8** に 1480 ℃の曲げ強さの混合等高線プロットを示す。圧縮強さに比べて粒度構成との相関性が少し低いが，熱間曲げ強さに

particle ratio increased from ④ to ⑥, the strength increased from 78 (the range of 70-80) to 97 MPa (more than 90). Figure 8 shows a triangle contour plot of the modulus of rupture at 1480 ℃. Although the correlation of the modulus with the particle size distribution is slightly weaker than that of the cold crushing strength, the increasing trend of the modulus is observed with the increase in the ratio of fine particle.

Figure 9 shows a triangle contour plot of the

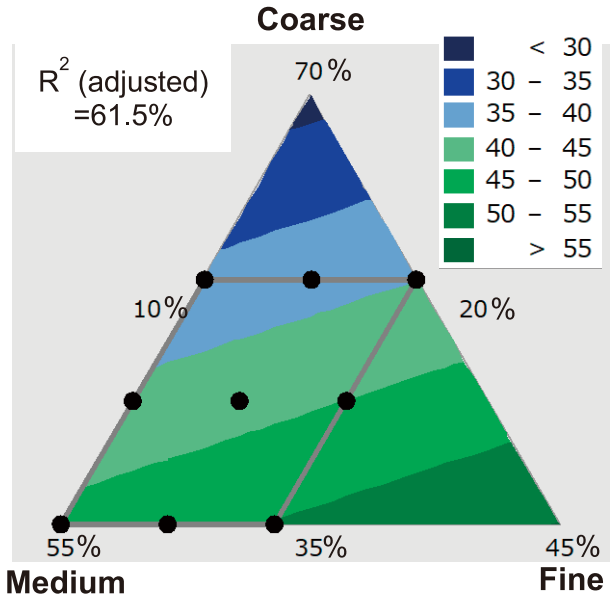

Fig. 9 Influence of particle size distribution on modulus of elasticity with triangle contour map.

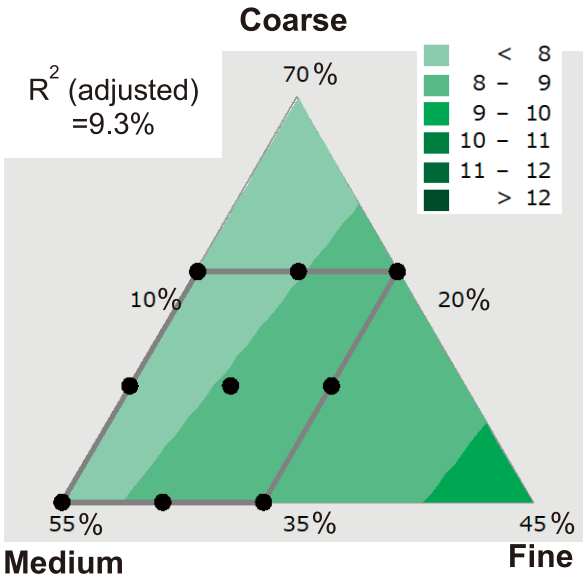

Fig. 10 Influence of particle size distribution on number of cycle to spall with triangle contour map.

おいても微粉割合増加に伴い，上昇する傾向が見られる。

図 9 に音速弾性率の混合等高線プロットを示す。粗粒割合の増加に伴い，低下する傾向が見られた。同じ微粉割合 17.5% で粗粒割合が⑧から②に増加した場合，音速弾性率は，50 GPa（45-50 の領域）から 35 GPa（35-40 の領域）に低下している。

耐熱衝撃性評価における剥落までの回数を**表 2**

modulus of elasticity which tends to decrease with increasing in the ratio of coarse particle. When the coarse particle ratio increased from ⑧ to ② at the same fine particle ratio of 17.5%, the modulus of elasticity decreased from 50 (the range of 45-50) to 35 GPa (the range of 35-40).

The number of cycles to spall as the results of the thermal shock resistance test is shown in **Table 2**. A triangle contour plot of the thermal shock resistance is shown in **Fig. 10**. The higher number means the

に示す。回数が多いほど，耐熱衝撃性が高いということになる。この結果に基づいて作成した混合等高線プロットを**図 10** に示すが，R^2（調整済み）が 9.3% と低く，粒度構成と耐熱衝撃性に相関性は見られなかった。

4　考察

4・1　成形体と焼成体のかさ比重と見掛気孔率に及ぼす粒度構成の影響

粗粒・微粉割合の増加に伴いかさ比重が増加し，見掛気孔率が低下した要因は 2 つあると考えられる。一つは，粗粒割合増加に伴う成形性の向上である。**表 3** 及び**図 11** に焼成前のかさ比重の結果を示し，粗粒割合の増加に伴い高くなり粗粒 55%，中粒 27.5%，微粉 17.5% の粒度構成②で最も高くなっている。**表 3** に各粒度構成① - ⑨の混練後坏土のタップ密度と成形体のかさ比重を示しているが

higher thermal shock resistance. The thermal shock resistance had no correlation to the particle size distribution with exhibiting low value of the adjusted R^2 of 9.3%.

4 Discussion

4•1 Influence of the particle size distribution on the density and porosity

There are two reasons why the bulk specific gravity increases and the apparent porosity decreases with increasing the ratios of coarse and fine particles. One is the improvement in moldability with the increase in the ratio of coarse particles. **Table 3** and **Fig. 11** show the results of measurements and a triangle contour plot of the bulk specific gravity before firing, respectively. The gravity increases with the increase in the ratio of coarse particle, and is highest in the particle size distribution ② with 55% coarse, 27.5% medium, and 17.5% fine particles. The tap density of the mixture was also highest in ②, indicating that the particle size distribution was optimal for the filling and moldability of the mixture.

Table 3　Tap density of mixture and bulk specific gravity before firing

Particle size distribution	①	②	③	④	⑤	⑥	⑦	⑧	⑨
Tap density of mixture g / cm^3	2.27	2.38	2.33	2.27	2.22	2.33	2.22	2.27	2.33
Bulk specific gravity / -	3.40	3.41	3.39	3.38	3.40	3.38	3.37	3.39	3.38

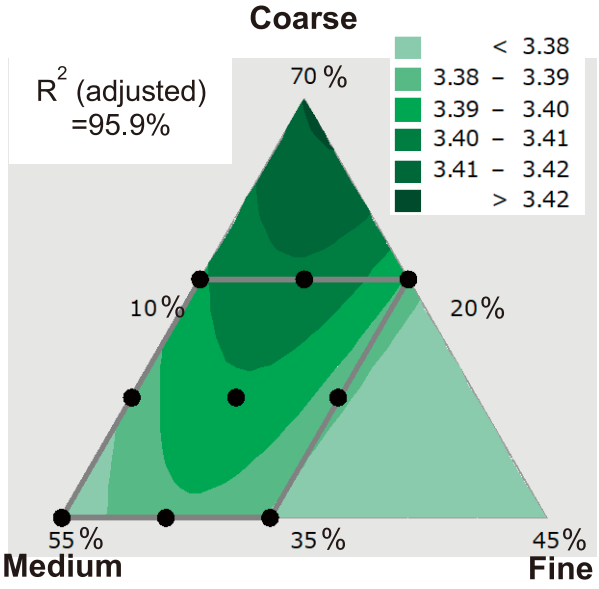

Fig. 11　Influence of particle size distribution on bulk specific gravity before firing with triangle contour map.

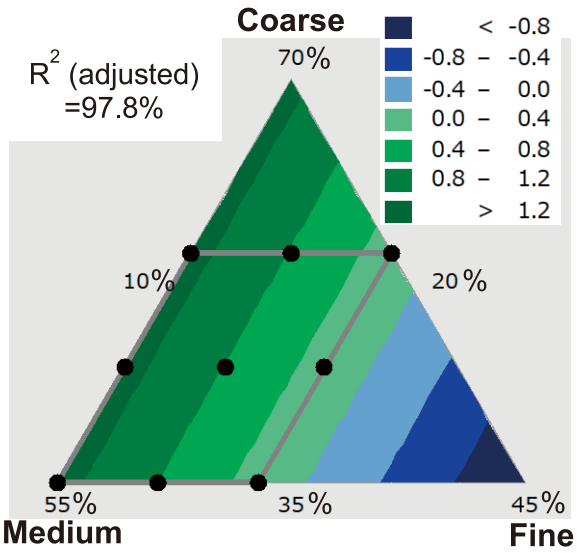

Fig. 12 Influence of particle size distribution on percentage dimensional change in molding direction with triangle contour map.

両方の値とも②が最も大きくなっており，坏土の充填性そして成形性に最適な粒度構成であったことを示している。もう一つは，微粉割合の増加に伴う焼成膨張の抑制である。**図 12** に焼成前後の成形方向の寸法変化率の混合等高線プロットを示し，微粉割合の増加に伴う寸法変化の低減を示している。これは微粉増加による焼結性の増進によるものと考えられる。**図 4** に示す微構造写真において微粉割合増加に伴いつまり①～③，④～⑥そして⑦～⑨へと微粉を介した結合が増加し，焼結が進行していることがわかる。また，焼結理論から，粒径が小さいほど焼結緻密化速度が高い[3] ことが知られている。粗粒割合増加に伴う成形性の向上，微粉割合増加に伴う焼成膨張の抑制により，粗粒･微粉割合が高い程，かさ比重が増加し，見掛気孔率が低下した。

4･2　粒度構成が与える物性（冷間圧縮強さ・熱間曲げ強さ・音速弾性率）への影響

冷間圧縮強さ・熱間曲げ強さが微粉割合増加に伴い，増大した要因は二つ考えられ，一つは，焼成体における焼結が進み，組織が強化されたこと，もう一つは，10 μm 以上の比較的大きな空隙（細

Another reason is the suppression of thermal expansion during firing with the increasing the ratio of fine particle. **Figure 12** shows the triangle contour plot of the dimensional change rate in the molding direction before and after firing, indicating a reduction in dimensional change with the increase in the ratio of fine particle. This is thought to be due to the increased sinterability by increasing the fine particle. In the micrographs shown in **Fig. 4**, the bonding through fine grain increases with increasing the ratio of fine particle in the particle distribution on the powder processing, from ① to ③, ④ to ⑥, and ⑦ to ⑨ with exhibiting the advancement of sintering, respectively. Indeed, the theory of sintering[3] clarified that high densification through sintering is facilitated to achieve by using the finer particle. With improving the moldability by increasing in the ratio of coarse particle and the suppression of thermal expansion by increasing in the ratio of fine particle, the higher bulk specific gravity and the lower apparent porosity were achieved in particle size distribution with the higher ratio of coarse and fine particles.

4･2 Influence of particle size distribution on the mechanical properties

There are two reasons why the cold crushing strength and hot modulus of rupture increased with the increase in the ratio of fine particle: one is increased sinterability during firing with resulting in the strengthened structure, and another is elimination

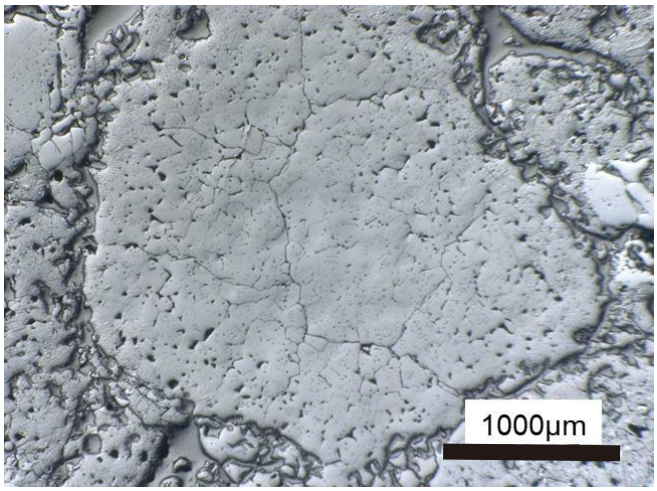

Fig. 13 Voids surrounding the magnesia coarse grain in the fired material with particle size distribution ①.

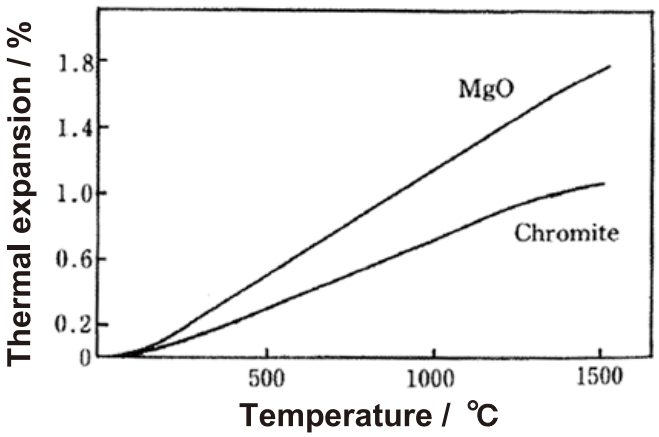

Fig. 14 Thermal expansion of magnesia raw materials and chromite[4].

孔）が減少したことである。

また，音速弾性率に関しては，**図 9** に示したように，粗粒割合の増加に伴い，弾性率が低下する傾向であった。これは，焼成時の膨張・収縮過程に形成される粗粒周囲の空隙が影響しているものと考えられた。実際に**図 13** に粒度構成①の焼成体における微構造写真に示しているように，マグネシア粗粒周囲に空隙が見られ，これは，焼成時に膨張した粗粒が，降温時に収縮したことにより，生じたものと考えられる。粗粒は，中粒・微粉に比べ加熱時の膨張代が大きく，冷却により周囲に空隙を生じ易いため，粗粒割合増加に伴い，空隙が多くなり，弾性率が低下したと考えられる。さらに，**図 14** に示すように，マグネシアはクロム鉱に比べ

of relatively large void(pore) with size of 10 μm or more.

As for the modulus of elasticity, there was a tendency to decrease with the increase in the ratio of coarse particle as shown in **Fig. 9**. The decrease in the modulus was thought to be caused by the formation of voids around the coarse particle which expands and contracts during the firing easily by affecting the temperature rise and drop. In the micrograph of the fired body with the particle size distribution ① as shown in **Fig. 13**, voids were actually observed at around the magnesia coarse grain, they were thought to be formed during firing in the manner described above. Degree of expansion and contraction during firing is higher in coarse particle than medium and fine particle. The coarse particle tends to form voids around it so the ratio of coarse particle increases, the more voids are formed with resulting in lowering of

熱膨張率が大きいため，マグネシア粗粒周囲の空隙は特に多くなり，弾性率のさらなる低下に寄与しているものと推定された。

4・3　粒度構成が与える耐熱衝撃性への影響

図 10 に示したように，粒度構成と耐熱衝撃性に相関性は見られなかった。その理由を考察するために熱衝撃損傷抵抗の指標となるR''''を以下の式[5]により求めた。

$$R'''' = \frac{E\gamma}{S^2(1-\upsilon)}$$

式中の破壊エネルギーγを一定とし，熱衝撃損傷抵抗を（E/S^2）で比較した（**表 2** 参照）。ここでEは音速弾性率，Sは 1480 ℃における曲げ強さの測定値をそれぞれ用いて計算した。粒度構成が（E/S^2）に与える影響を示す混合等高線プロットを**図 15** に示すように，R^2（調整済み）は 34.6% となり，低い相関性を示した。このことにより，耐熱衝撃性と粒度構成に相関性が見られなかったと考えられる。

the modulus of elasticity. Furthermore, since magnesia has a larger thermal expansion rate than chromite as shown in **Fig. 14**, the voids formed around the magnesia coarse particle must be abundant with presuming their contribution to a further decrease in the modulus of elasticity.

4·3 Influence of particle size distribution on the thermal shock resistance

As shown in **Fig. 10**, no correlation was found between the particle size distribution and the thermal shock resistance in the magnesia-chrome bricks. To consider the reason for this, the indicator of thermal shock damage resistance, R'''', was calculated by the following equation [5].

$$R'''' = \frac{E\gamma}{S^2(1-\upsilon)}$$

Suppose the fracture energy γ in the equation is constant, the thermal shock damage resistance is determined by the term (E/S^2) (see **Table 2**). Here, E and S are the modulus of elasticity and the modulus of rupture at 1480 ℃, respectively, and the measured values of them were used for calculation. The contour plot showing the effect of particle size distribution on (E/S^2) is shown in **Fig. 15**, and R^2 (adjusted) was

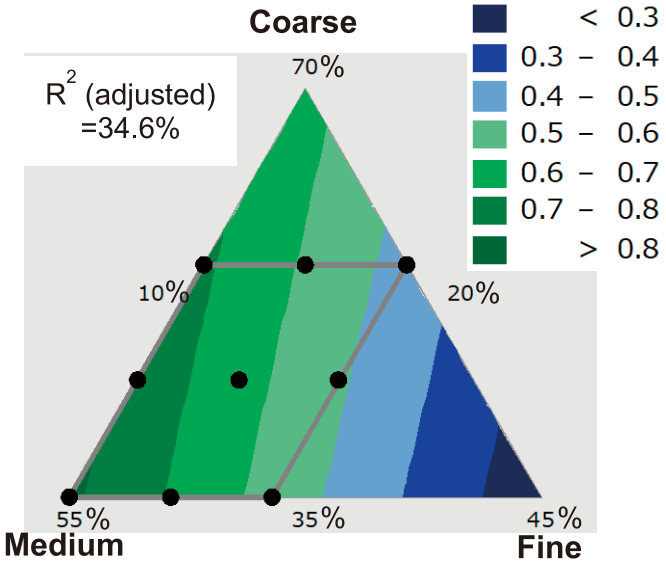

Fig. 15　Influence of particle size distribution on E/S² with triangle contour map.

5　まとめ

今回，マグクロれんがの粒度構成が物性に与える影響について調査した。

・粗粒割合の増加に伴い，成形性が向上し，微粉割合の増加に伴い，焼結性が増進，焼成膨張が抑制された。その結果，粗粒及び微粉割合のうち後者が高い場合高かさ比重，低見掛気孔率となった。

・強度は微粉割合の増加に伴い向上し，音速弾性率は，粗粒割合の増加に伴い低下した。

・耐熱衝撃性は，粒度構成との相関性は見られなかった。

文　献

1）玉木健之：耐火物，**44** [4] 226-237（1992）.

2）北井恒雄，大崎博右，山本哲夫：耐火物，**45** [7] 414-420 (1993).

3）吉田英弘：まてりあ，**58** [11] 677-683（2019）.

4）耐火物技術協会：耐火物手帳　改訂 12 版，耐火物技術協会（2015）p.150.

5）耐火物技術協会：耐火物手帳　改訂 12 版，耐火物技術協会（2015）p.101.

本論文は以下の報文に加筆・再構成して転載したものである。

岸本他：第 11 回鉄鋼用耐火物研究会講演会報告集，耐火物技術協会（2023）pp.86-93

34.6%, showing a weak correlation. From this, it is believed that no correlation was found between the thermal shock resistance and the particle size distribution.

5 Conclusions

In this study, we have investigated influence of particle size distribution on the properties of magnesia-chrome bricks.

- With the increase in the ratio of coarse particle, the moldability improved, and with the increase in the ratio of fine particle, the sinterability increased and the thermal expansion during firing was suppressed. As a result, when the ratio of coarse particle and fine particle was high, the bulk specific gravity was high and the apparent porosity was low.
- The strength improved with the increase in the ratio of fine particle, and the modulus of elasticity decreased with the increase in the ratio of coarse particle.
- No correlation was found between thermal shock resistance and particle size distribution.

References

1) K. Tamaki: TAIKABUTSU, **44** [4] 226-237 (1992)

2) T. Kitai, H. Osaki and T. Yamamoto: TAIKABUTSU, **45** [7] 414-420 (1993)

3) H. Yoshida: Materia Japan, **58** [11] 677-683 (2019)

4) Technical Association of Refractories, Japan eds.: Refractories Handbook Revised 12th Edition, Technical Association of Refractories, Japan (2015) p.150.

5) Technical Association of Refractories, Japan eds.: Refractories Handbook Revised 12th Edition, Technical Association of Refractories, Japan (2015) p.101.

This paper is reprinted with some additions and reconstructions to the following paper:
Kishimoto et al.: Proceedings of the 11th Symposium on Refractories for Iron and Steel, Technical Association of Refractories, Japan (2023) pp.86-93.